NUCLEAR SCIENCE AND TECHNIQUES **26**, S10312 (2015)

Hydriding properties of uranium alloys for purposes of searching for new hydrogen storage materials*

Michio Yamawaki,[1,†] Takuya Yamamoto,[1] Yuji Arita,[1] Fumihiro Nakamori,[1] Kazuhito Ohsawa,[2] and Kenji Konashi[3]

[1]*Research Institute of Nuclear Engineering, University of Fukui, 1-2-4, Kanawa-cho, Tsuruga, Fukui, 914-0055, Japan*
[2]*Research Institute for Applied Mechanics, Kyushu University, 6-1 Kasuga-koen, Kasuga, Fukuoka, 816-8580, Japan*
[3]*Institute for Materials Research, Tohoku University, 2145-2 Narita-cho, Oarai, Higashi-Ibaragi-gun, Ibaragi, 311-1313, Japan*

(Received May 11, 2014; accepted in revised form June 27, 2014; published online December 20, 2014)

Hydriding properties of uranium alloys have been studied to search for new hydrogen storage materials to be applied to hydrogen energy systems. Application of uranium-base hydrogen storage materials can be expected to alleviate the risk, as well as to reduce the cost incurred by globally-stored large amounts of depleted uranium left after uranium enrichment. Various uranium alloys have been examined in terms of hydrogen absorption-desorption properties, among which UNiAl intermetallic compound showed promising characteristics, such as lower absorption-desorption temperatures and better anti-powdering strength. First principle calculation has been carried out on UNiAl hydride to predict the change of crystal structure and the lattice constant with increasing hydrogen content, which showed this calculation to be promising in predicting candidates for good hydrogen absorbers.

Keywords: Depleted uranium, Hydrogen storage material, Uranium alloys, UNiAl intermetallic compound, First principles calculation

DOI: 10.13538/j.1001-8042/nst.26.S10312

I. INTRODUCTION

The hydrogen energy system requires a large-scale stationary storage facility at hydrogen generation plants. Common forms that hydrogen can be stored in include compressed gas, cryogenic liquid, and metal hydrides [1]. Each of these storage methods has advantages and disadvantages, as well as requires some degree of energy consumption, that mainly arises in gas compression, maintaining cryogenic temperature, or heating metal hydrides for desorption, respectively. One of the advantages of using metal hydrides is the inherent safety. It only requires moderate pressure when storing and passively contains hydrogen in case of power loss. One disadvantage of metal hydrides for mobile storage is limited mass energy density. This is not a practical concern to the stationary system, or rather, they may produce as high a volume energy density as other methods. The cost of the metal hydride storage system would largely depend on the material and the operational temperature range. Yamawaki *et al*. have previously proposed a surplus electricity storage system utilizing depleted uranium as a base storage material [2, 3].

Depleted uranium has been produced abundantly as waste from the uranium enrichment process but has never been used effectively. It is usually stored idly as uranium fluoride gas or in solid form. On the contrary, uranium is one of the highest capacity hydrogen storage materials. It readily absorbs hydrogen to form uranium hydride, UH_3, at room temperature and discharges hydrogen reversibly at an elevated temperature. In fact, uranium has commonly been used to store tritium, the radioactive isotope of hydrogen, since the room temperature desorption pressure is low enough to securely contain it. On the other hand, discharging hydrogen at a dissociation pressure of 10^5 Pa requires heating the hydride up to about 700 K. The discharging temperature is rather high for hydrogen storage applications incurring significantly large operational energy loss. Further, uranium undergoes large volumetric expansion upon hydrogenation due to the large change in crystal structure, which causes severe powdering of the material leading to low thermal conductivity and increasing pyrophilicity. Hydrogen absorption-desorption properties of various uranium alloys have been studied in order to find alloys with improved anti-powdering capacity as well as high desorption pressure by Yamawaki and co-workers [3–10].

The objective of this paper is to summarize the status and approach development of uranium alloys as hydrogen storage material.

II. HYDROGEN ABSORPTION-DESORPTION PROPERTIES OF URANIUM ALLOYS

A. U-Zr and U-Ti alloys

Hydrogen absorption-desorption properties and the reactivity with air of U-Zr and U-Ti alloys were investigated for use in depleted uranium based energy storage systems as well as for tritium storage systems [3–8]. Some of the U-Zr and U-Ti alloys have hydrogen absorption-desorption properties as good as those of uranium. Further, the pyrophilicity of Zr- or Ti-rich uranium alloys is more moderate than that of U-rich

* Supported by Grants-in-Aid for Scientific Research (No. 25420903) from the Ministry of Education, Culture, Sports, Science and Technology of Japan and Japan Industrial Location Center
† Corresponding author, yamawaki@u-fukui.ac.jp

TABLE 1. Hydrogen capacity and powdering behavior of U-Zr and U-Ti alloys [3]

Alloy	H capacity [H]/[UM$_x$]		Powdering after cycling	
	Maximum	Rechargeable	Diameter (μm)	Abs.-Des. Cycles
U (ref.)	3	3	20–30	2–3
$UZr_{1/2}$	4	3	–[b]	19.5
UZr	5	2.7	100	11
UZr_2	6.5	1–3	1–400	12.5
$UTi_{1/2}$	3.7	2.7 – 3.7[a]	–[b]	13
UTi	5	2.3 – 4.5[a]	–[b]	14.5
UTi_2	7	1.2 – 5.5[a]	1–10	12

[a] The higher capacities with utilizing low UTi_2H_x phase plateaus;
[b] Fine powder except a few granules.

alloys due to the higher resistance against powdering upon hydrogenation [3, 7]. Table 1 summarizes the hydrogen storage capacities of U-Zr and U-Ti alloys [3]. On hydrogenation, U-Zr and U-Ti alloys decompose into UH_3 and ZrH_x ($x < 2$) and UH_3 and UTi_2H_x ($x < 5$) phases, respectively, so that *P-c-T* diagrams consist of the plateau regions of corresponding phases. Because of low equilibrium H pressure of ZrH_x phases, the rechargeable hydrogen capacities of U-Zr alloys depended on the fraction of UH_3 phase (or U content in the alloy), except UZr_2 where the UH_3 region becomes smaller after cycles. In U-Ti alloys the ternary phase UTi_2H_5 formation consumes some uranium to narrow the UH_3 plateau region, while utilizing the lower pressure UTi_2H_5 plateau can extend the rechargeable capacity. Alloying U with Zr or Ti basically keeps the equilibrium pressure of UH_3, while powdering is greatly reduced, especially with high content of Zr or Ti. Table 1 also shows the degree of powdering after up to $\approx$ 20 hydrogen absorption-desorption cycles [3]. UZr, UZr_2, and UTi_2 alloys showed significant resistance against severe disintegration into fine powders even after more than 10 cycles. UZr especially possess a good balance of large capacity and high resistance against powdering.

B. U-Mn, U-Fe and U-Ni alloys

Uranium-rich intermetallic compounds, namely U_6M (M = Fe, Mn, Ni), commonly forms in these binary systems. Cubic $MgCu_2$-type UM_2 phase is the only other intermetallic phase in the U-Mn and U-Fe systems, while four additional phases form in the U-Ni system, including UNi_5 and UNi_2 of known $AuBe_5$- and Cu_2Mg-type crystal structure, respectively, as well as U_5Ni_7 and U_7Ni_9. The hydrogen absorption properties of these compounds have been studied [6, 10], where none of the alloys except the U_6M-type compounds were found to be reactive to hydrogen. All U_6M type compounds absorbed hydrogen to form UH_3 and the corresponding UM_2 phases. The *P-c-T* isotherms of these alloys basically consist of a wide single plateau of UH_3. As shown in Fig. 1, the plateau pressures in these U_6M alloys are all higher than pure U. Among the alloys, U_6Fe has the highest desorption pressure.

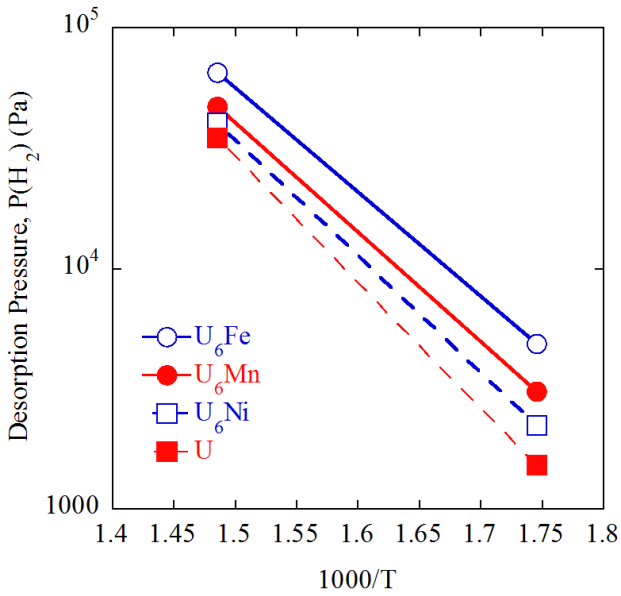

Fig. 1. (Color online) Hydrogen desorption pressure of U_6M type alloys in comparison with uranium.

C. UCo

UCo, one of the six known intermetallic compounds in the U-Co system, is known to form $UCoH_{2.7}$ [9, 11]. Our study on the hydrogen absorption—desorption behaviors of the compound has shown that there are two stages of desorption reactions at higher temperatures than 473 K, while only a single stage was observed below 423 K [9]. UCo readily absorbs hydrogen to form $UCoH_{2.7}$ at temperature below 423 K under the hydrogen pressure of 10^5 Pa. It simply dehydrogenates reversibly at 423 K, while two-phases of UH_3 and UCo_2, appear during the desorption of $UCoH_{2.7}$ above 473 K. This is due to the following two competing reactions:

$$UCoH_{2.7} = 0.5UCo_2 + 0.5UH_3 + 0.6H_2, \quad (1)$$

$$UCoH_{2.7} = UCo + 1.35H_2. \quad (2)$$

The standard Gibbs energy changes, ΔG_1^0 and ΔG_2^0, for reactions (1) and (2), respectively, as functions of T and hydrogen pressure, p, were estimated as follows

$$\Delta G_1^0 = 8.4 \times 10^4 - 174T + 0.6RT\ln(p/p_o), \quad (3)$$

$$\Delta G_2^0 = 7.4 \times 10^4 - 147T + 1.35RT\ln(p/p_o), \quad (4)$$

here, p_o is the standard pressure (101 325 Pa), R is the gas constant (8.3 J/(mol K)), and each Gibbs energy is calculated per mole of $UCoH_{2.7}$. Fig. 2 plots the ΔG_1^0 and ΔG_2^0 vs. T in lines with unfilled and filled symbols, respectively, for two cases of p. Solid lines with circles are for $p = 10^4$ Pa, while broken lines with squares are for $p = 10^5$ Pa. For lower p ($= 10^4$ Pa), ΔG_2^0 is lower than ΔG_1^0 over a wide temperature

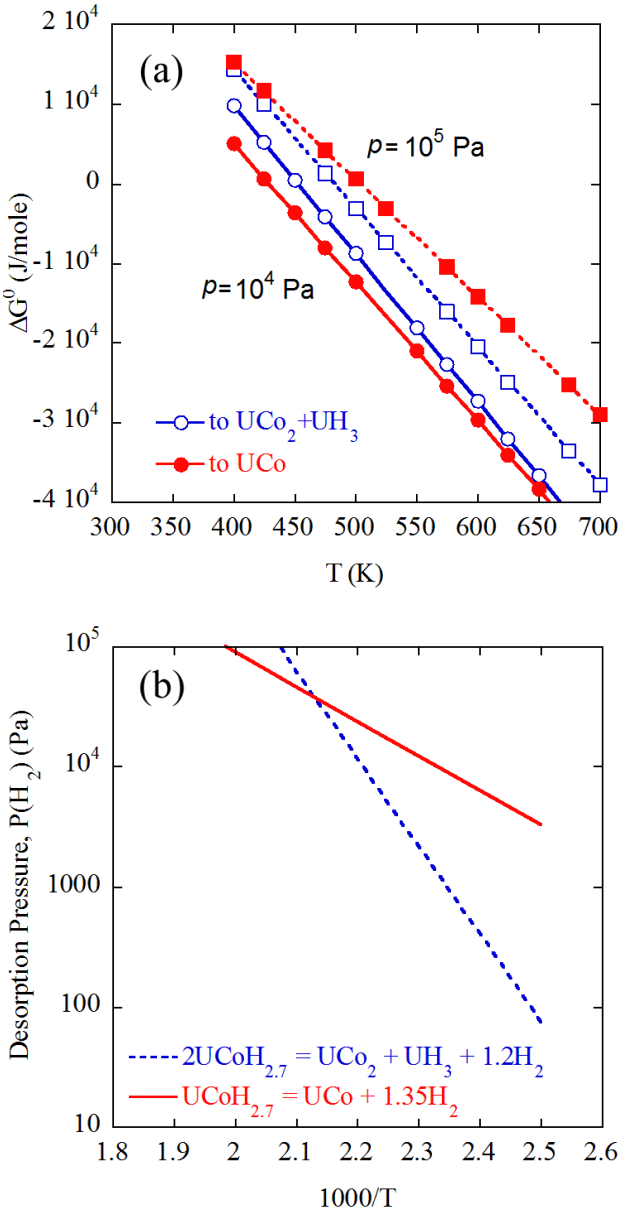

Fig. 2. (Color online) (a) Standard Gibbs energy changes of two competing reactions on dehydrogenation of $UCoH_{2.7}$ for the hydrogen pressure p of 10^4 Pa (Solid lines) and 10^5 Pa (dotted lines). The reaction (1) to decompose into two phases and (2) to reverse to UCo are shown in the lines with unfilled and filled symbols, respectively; (b) Equilibrium desorption pressures based on the enthalpy and entropy changes given in Ref. [9].

range below 650 K, while at $p = 10^5$ Pa, ΔG_2^0 is higher at $T > 400$ K. This results in the observation of a single stage reaction (2) at lower T and lower p, while two stages, including the decomposition into UCo_2 and UH_3, result at higher T and higher p.

While desorption operations may be limited in the p range, UCo can reversibly absorb and desorb hydrogen at a relatively low temperature of 423 K with the desorption pressure significantly higher than that of UH_3.

D. UNiAl and other Fe_2P-type uranium compounds

UNiAl intermetallic compounds have a hexagonal Fe_2P-type (or also known as ZrNiAl-type) crystal structure. As illustrated in Fig. 3(a), the unit cell consists of a stack of two kinds of planes, one with three U and one Ni atom and the other with three Al and two Ni atoms. Table 2 shows more details of the atomic positions in terms of Wyckoff's notations and representative partial coordinates. In the original crystal structure, there are two U atom triangles per unit cell, which with two Ni atoms on the adjacent planes make tetrahedral interstitial sites sharing the triangle, as illustrated also in Fig. 3(a). At hydrogen pressures below 10^5 Pa, UNiAl absorbs up to two hydrogen atoms per unit cell, or around 0.7 H per UNiAl formula unit (F.U.) (H/F.U.) [11–13]. The neutron diffraction study of a deuteride, $UNiAlD_{0.7}$, showed that D atoms occupy the U_3Ni_1-type interstitial sites. At a higher hydrogen pressure it can absorb up to around 2 H/F.U. [14]. Yamamoto *et al.* showed that the crystal structure of $UNiAlH_{2.2}$ or $UNiAlD_{2.2}$ has significantly different atomic positions while retaining basic hexagonal structure. Table 2 also shows the detailed crystal structure of the deuterides, including the atomic positions. In $UNiAlD_{2.2}$ formation the uranium positions shift to increase x in the representative coordinate, (x, 0, 1/2), of 3g position. Aluminum atoms also move within the plane in the same direction as that of U atoms, while Ni atoms in the 1b position moves along the c-axis to $z = 0$ from $z = 1/2$. These changes are illustrated in Fig. 3(b), 3(c), and 3(d) show U and Ni atom positions on the $z = 1/2$ plane for UNiAl, $UNiAlD_{0.7}$, and $UNiAlD_{2.2}$, respectively. U atoms shift to increase x from 0.580 to 0.592 and 0.659 makes the U triangle, forming an U_3Ni_1-type interstitial site larger by 4% and 17%, respectively, which presumably is required to secure the U-D distance. It is noticeable that these shifts also make the other U triangles similar equilateral ones. Deuterium occupying sites are also shown in Fig. 3(c) and 3(d) with three different triangle symbols for $U_3Ni_1^I$-type D(1), U_3Al_1-type D(2), and $U_3Ni_1^{II}$-type D(3) sites, respectively. The final D site structure suggests that it is the atomic position shifts that really enabled this compound to accept around 6 hydrogen atoms per unit cell.

Hydrogen desorption isotherms of UNiAl have been studied in detail by Yamanaka *et al.* [14]. Fig. 4 shows the hydrogen desorption pressures at two plateau regions, between α and β and β and γ phases, corresponding to the following nominal reactions, respectively:

$$UNiAl + 1/3H_2 = UNiAlH_{0.66}, \quad (5)$$

$$UNiAlH_{0.66} + 2/3H_2 = UNiAlH_2, \quad (6)$$

here, H compositions are all nominal values based on the number of H atoms occupying the 4h site and the 4h, 3g, and 2e sites for β and γ phases, respectively. The figure indicates that the desorption pressure for the reaction (6) reaches around 10^5 Pa at 400 K, which is sufficiently high for hydrogen storage use of the material. The lower plateau reaches

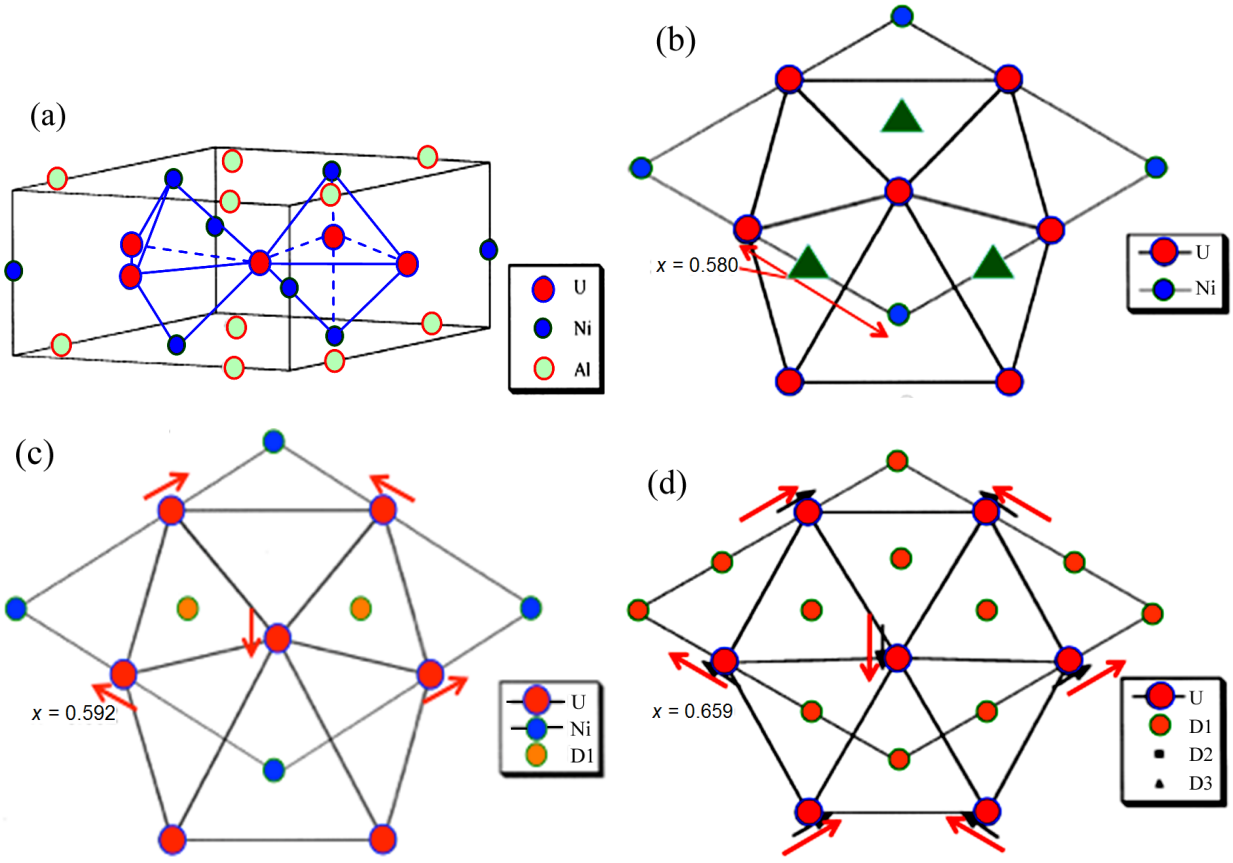

Fig. 3. (Color online) (a) Crystal structure of UNiAl showing four U_3Ni^I-type tetrahedral sites; (b) atomic arrangements on the U plane at $z = 1/2$ in (a) UNiAl, (c) $UNiAlD_{0.7}$ and (d) $UNiAlD_{2.2}$.

10^5 Pa at around 550 K, which may be acceptable, while using only higher plateau region allows recycling of around 2/3 of the total hydrogen capacity.

III. FIRST PRINCIPLES CALCULATIONS BASED APPROACH TO NEW URANIUM HYDRIDES

There are around 20 known ternary uranium compounds of ZrNiAl-type crystal structure. A few of them, as well as their quaternary mixtures have been investigated in terms of hydrogen absorption properties [16–19]. Of all those that have been examined, UNiAl has the largest hydrogen capacity at around 2H/F.U., while that all others hold no more than around 1H/F.U. This suggests that the relocations of metallic atoms described in the previous section are of great importance to the large hydrogen capacity. In searching for other ZrNiAl-type U intermetallic compounds that can hold large amount of hydrogen, knowing the possibility of such atomic relocations would provide a very helpful guidance. First principle calculations of potential hydrides can be used to examine that possibility. To start off we have carried out the calculations of $UNiAlH_n$ with n up to 2, which shows that the crystal unit shown in Fig. 3(a) holds up to 6 H atoms, to learn how the theory can inform us of the potential hydrogenation.

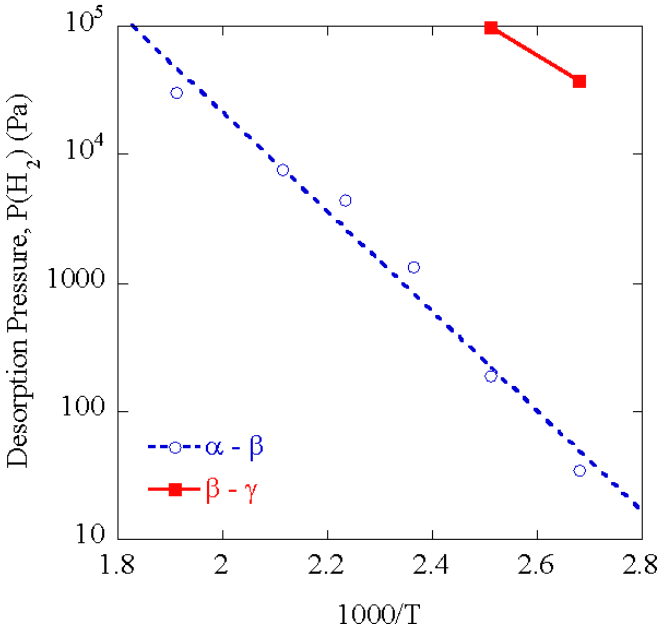

Fig. 4. (Color online) Hydrogen desorption pressures of UNiAl reproduced from *P-x-T* diagram in Ref. [14].

TABLE 2. Crystal structures of UNiAl and its deuterides

		UNiAl [11]		$UNiAlD_{0.7}$ [10]		$UNiAlD_{2.2}$ [11]	
Phase in Ref. [14]		α		β		γ	
DFT model in Section III		Structure A				Structure B	
Lattice constants	a	0.6732		0.6962		0.7171	
	c	0.4036		0.3992		0.3976	
Wyckoff's for sg 189, P62m		Coordinates & occupancy					
U	3g	(0.580, 0, 1/2)	1	(0.592, 0, 1/2)	1	(0.659, 0, 1/2)	1
Ni (1)	1b	(0, 0, 1/2)	1	(0, 0, 1/2)	1	—	
Ni (1')	1a	—		—		(0, 0, 0)	1
Ni (2)	2c	(1/3, 2/3, 0)	1	(1/3, 2/3, 0)	1	(1/3, 2/3, 0)	1
Al	3f	(0.219, 0, 0)	1	(0.239, 0, 0)	1	(0.347, 0, 0)	1
D (1)	4h	—		(1/3, 2/3, 0.488)	1/2	(1/3, 2/3, 0.436)	0.40
D (2)	3g	—		—		(0.331, 0, 1/2)	1
D (3)	2e	—		—		(0, 0, 0.43)	1/2
D (4)	6j	—		—		(0.207, 0.233, 0)	0.09
D (5)	3f	—		—		(0.577, 0, 0)	0.15

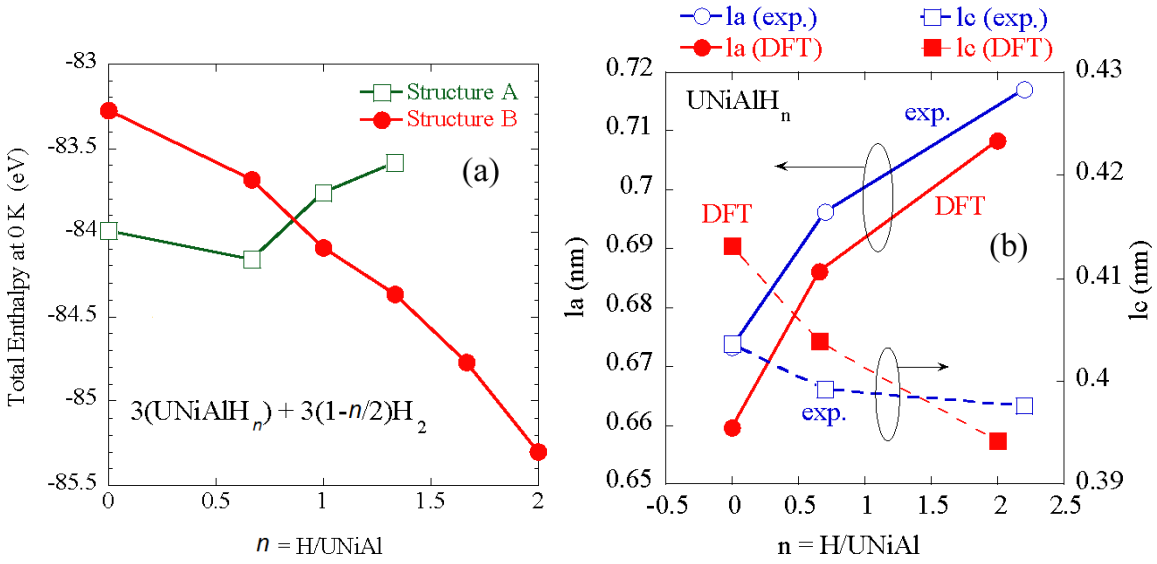

Fig. 5. (Color online) (a) Total enthalpy of $3(UNiAlH_n) + 3(1-n/2)H_2$ system from the DFT calculations as a function of n in two metallic atom structures; (b) the lattice constants, la and lc, as a function of H concentration, n (= H/UNiAl) for both of DFT and experiments.

The first-principle calculations based on the density-functional theory (DFT) are performed using the Vienna ab-initio simulation package, VASP, with generalized gradient approximation and projected augment wave potentials [20, 21]. We employed a hexagonal unit-cell containing three UNiAl formula units as shown in Fig. 3(a) with its Brillouin zone with 3 3 5 k-point sampling using the Monkhorst-Pack scheme [22]. The plane-wave energy cutoff is 350 eV. Atomic positions and cell size relaxations are iterated until the total energy between two ionic steps is smaller than 0.0005 eV.

Two structures of metallic atoms were considered in the calculations. Structure A is based on the original UNiAl structure, while Structure B is based on the experimentally observed $UNiAlD_{2.2}$ crystal structure. Key difference is that 1/3 of Ni atoms locate in 1(b) (0, 0, 1/2) positions in Structure A but in 1(a) (0, 0, 0) in Structure B. Hydrogen atoms are initially placed in positions where D atoms were found to occupy in $UNiAlD_{0.7}$ and $UNiAlD_{2.2}$. Details of calculation will be reported in the future, while the preliminary results of DFT calculations have supported various observations in the experiments. For example, Fig. 5(a) shows the total enthalpy of the $3(UNiAlH_n) + 3(1-n/2)H_2$ system from the DFT calculations as a function of n in two metallic atom structures. Structure A has lower energy for $n \leq 2/3$ (2 H atoms in the crystal unit shown in Fig. 3(a)), while for $n \geq 1$, structure B becomes more energy favored. The most stable crystal structure in DFT calculations also supports the observed shifts in atomic positions of U and Al along the x-axis (listed in Table 2). Fig. 5(b) plots the lattice constants, la and lc, as a function of H concentration, n (= H/UNiAl) for both DFT

and experiments. The characteristic trends of the changes in the lattice constants show an increas in la while decreasing in lc with increasing n, are qualitatively in good agreement between the calculation and experiments. Although these are still preliminary results, as quantitative comparisons between calculations and experiments need to be examined in more detail, the results at least qualitatively support the experimental trends suggesting that the approach would be able to give a list of candidates for good hydrogen absorbers.

IV. CONCLUSION

A hydrogen energy age is coming soon, where metal hydride will be used as a hydrogen storage material. The alloy of uranium with Zr, Ti, Mn, Fe, Ni, and Co each has been examined in terms of its potential to be used as a hydrogen storage material, since large amounts of depleted uranium will become available. Each alloy has advantages and disadvantages, while the UNiAl intermetallic compound has been evaluated as a considerably promising material on account of relatively low working temperatures and good anti-powdering strength. First principles calculation has been carried out on $UNiAlH_x$ to estimate the change in crystal structure and lattice constants with changing hydrogen content. The results have supported the experimental trends, suggesting the present approach to be promising in giving a list of candidates for good hydrogen absorbers.

ACKNOWLEDGEMENTS

The authors thank Mr. Kunihiro Ito of the Nuclear Development Company for supplying uranium sample used to produce the UNiAl specimen of this study.

[1] Tamura H. Hydrogen storage alloys—fundamentals and frontier technologies. Tokyo: NTS Inc., 1998, 1–741. (in Japanese)
[2] Yamawaki M, Ito H, Yamamoto T. Electricity storage system-a possibility to use depleted uranium. Genshiryoku Kogyo, 1995, **41**: 27–33. (in Japanese)
[3] Asada K, Ono K, Yamawaki M, *et al*. Hydrogen absorption properties of uranium alloys. J Alloy Compd, 1995, **231**: 780–784. DOI: 10.1016/0925-8388(95)01717-8
[4] Yamawaki M, Suwarno H, Yamamoto T, *et al*. Hydrogenated actinide alloys as innovative fission reactor fuel and hydrogen storage materials. CIMTEC1999, Firenze, Italy, 1999.
[5] Konashi K and Yamawaki M. Environmentally friendly application of hydrides to nuclear reactor cores. Adv Appl Ceram, 2012, **111**: 83–88. DOI: 10.1179/1743676111Y.0000000051
[6] Yamamoto T, Supardjo T, Yamawaki M, *et al*. Storage of hydrogen isotopes in uranium alloys. Fusion Technol, 1988, **14**: 764–768.
[7] Yamamoto T, Yoneoka T, Yamawaki M, *et al*. Development of tritium processing material – A U-Zr alloy as a promising tritium storage material. Fusion Eng Des, 1989, **7**: 363–367. DOI: 10.1016/S0920-3796(88)80025-5
[8] Yamamoto T, Tanaka S, Yamawaki M. Hydrogen absorption-desorption properties of UCo. J Nucl Mater, 1990, **170**: 140–146. DOI: 10.1016/0022-3115(90)90405-C
[9] Yamamoto T, Kayano H, Yamawaki M, *et al*. Hydrogen absorption-desorption properties of UCo. J Less-Common Met, 1991, **172–174**: 71–78. DOI: 10.1016/0022-5088(91)90434-6
[10] Ito H, Yamaguchi K, Yamawaki M, *et al*. Hydrogen absorption properties of U_6Mn and U_6Ni. J Alloy Compd, 1998, **271–273**: 629–631. DOI: 10.1016/S0925-8388(98)00174-1
[11] Andreev A V, Bartashevich M I, Deryagin A V, *et al*. Influence of Hydrogen on the Magnetic Properties of the U-Co System. Phys Status Solidi A, 1986, **98**: K47–K51. DOI: 10.1002/pssa.2210980148
[12] Yamamoto T, Kayano H, Yamawaki M. Crystal structure of hydride and deuteride of unial. J Alloy Compd, 1994, **213–214**: 533–535. DOI: 10.1016/0925-8388(94)90981-4
[13] Yamamoto T, Ishii Y, Kayano H. Deuterium absorption properties and crystal structure of UNiAl. J Alloy Compd, 1998, **269**: 162–165. DOI: 10.1016/S0925-8388(98)00221-7
[14] Yamanaka S, Iguchi T, Fujita Y, *et al*. Study on the hydrogen solubility in UNiAl. J Alloy Compd, 1999, **293–295**: 52–56. DOI: 10.1016/S0925-8388(99)00300-X
[15] Drulis H, Petrynski W, Stalinski B, *et al*. Hydrogen absorption properties of selected uranium intermetallic compounds. J Less-Common Met, 1982, **83**: 87–93. DOI: 10.1016/0022-5088(82)90172-2
[16] Jacob I, Hadari Z, Reilly J J. Hydrogen absorption in ANiAl (A ≡ Zr, Y, U). J Less-Common Met, 1984, **103**: 123–127. DOI: 10.1016/0022-5088(84)90366-7
[17] Raj P, Sathyamoorthy A, Shashikala K, *et al*. The hydriding behaviour of $U(Fe_{1-x}\ Ni_x)$ Al system ($0 \leqslant x \leqslant 0.75$) and 12x x magnetic studies on $U(Fe_{1-x}\ Ni_x)AlH_{0.8}$. J Alloy Compd, 2000, **296**: 20–26. DOI: 10.1016/S0925-8388(99)00525-3
[18] Maskova S, Havela L, Danis S, *et al*. Onset of magnetism stimulated by H absorption in UNiAl-UFeAl. J Phys Conf Ser, 2011, **303**: 012011. DOI: 10.1088/1742-6596/303/1/012011
[19] Raj P, Sathyamoorthy A, Dhar S K, *et al*. Effect of deuterium absorption on the heavy-fermion compound UPdIn. Phys Rev B, 2002, **66**, 214420. DOI: 10.1103/PhysRevB.66.214420
[20] Kresse G and Hafner J. Ab initio molecular dynamics for liquid metals. Phys Rev B, 1993, **47**: 558–561. DOI: 10.1103/PhysRevB.66.214420
[21] Kresse G and Furthmueller J. Efficient iterative schemes for ab initio total-energy calculations using a plane-wave basis set. Phys Rev B, 1996, **54**: 11169–11186. DOI: 10.1103/PhysRevB.54.11169
[22] Monkhorst H J and Pack J D. Special points for Brillouin-zone integrations. Phys Rev B, 1976, **13**: 5188–5192. DOI: 10.1103/PhysRevB.13.5188